

# The Wigner molecule in a 2D quantum dot

**N. Akman** \*and **M. Tomak** †

Middle East Technical University, Department of Physics,  
06531 Ankara, Turkey

## Abstract

The charge density and pair correlation function of three interacting electrons confined within a two-dimensional disc-like hard wall quantum dot are calculated by full numerical diagonalization of the Hamiltonian. The formation of a Wigner-molecule in the form of equilateral triangular configuration for electrons is observed as the size of the dot is increased.

PACS Numbers: 73.20.Dx, 73.61.-r

Keywords: Quantum dot, Wigner molecule, low dimensional systems.

---

\*E-mail address: akman@newton.physics.metu.edu.tr

†E-mail address: tomak@rorqual.cc.metu.edu.tr

# 1 Introduction

Advances in nanostructure technology have allowed the lateral confinement of a two dimensional electron gas (2DEG) by means of suitably shaped gate electrodes or by etching techniques [1]. These confined systems having a discrete energy spectra are commonly called zero dimensional systems or quantum dots [2-9]. The motion of electrons in a quantum dot is quantized in all three spatial directions. However, if the quantization in the vertical direction is much stronger than the quantization in the in-plane directions, a quantum dot could be treated as disc-like 2D system where electrons have significant freedom along x- and y- directions.

Experimentally, the number of electrons confined in a quantum dot could be varied over a considerable range by changing the gate voltage applied. Quantum dots containing as few as 2, 3 or 4 electrons have already been realized and investigated by optical absorption experiments [6,9]. In these quantum dots or artificial atoms the Coulomb interaction between the electrons is very important for understanding their quantum mechanical properties. Especially correlations among electrons are crucial since their effects influence the spectral [10-14] and transport properties [15-17] of quantum dots.

So far, various analytical techniques have been devised for handling the electron correlations in quantum dot systems. One of these techniques include the solution of the many particle Schrodinger equation [18]. In this three dimensional approach, interacting electrons in non-parabolic quantum dot systems have been investigated using the formalism of Hylleraas [19] where interelectron coordinates are built into the wavefunction explicitly. By comparing Hylleraas and Hartree-Fock type results, in [18], it is shown how the charge redistributions, attributable to correlation interactions, affect ground and excited state energies and electron confinement in isolated and coupled two quantum dot systems. One- and two- electron ground state energies of a silicon sphere embedded in an amorphous silicon dioxide matrix [20] have been calculated as a function of sphere size. The electron-electron interaction and polarization effects in that study have been treated by perturbation.

A great deal of interest has also gone into analytical investigation of correlation effects in 2D quantum dot systems. Comparison of energies, pair correlation functions, and particle densities of the singlet and triplet ground state of quantum dot helium in a magnetic field has been investigated in [14] by using Hartree, Hartree-Fock, and exact diagonalization methods. The HF results for the triplet ground state were found to be in very good agreement with the exact diagonalization results, proving the importance of the exchange interaction. On the other hand, the exact results for the singlet state have disagreements with the HF results. In

[14] it has been shown that the disagreement between two results arises due to the electron correlations which are neglected in the Hartree-Fock approximation. However, most of the work performed on the electron-electron correlations in quantum dots placed in a magnetic field [6,8,21], as well as transport experiments [22] and far-infrared spectroscopy [23] has been based on a two dimensional quantum dot with parabolic type confinement potential.

Typically the lateral confinement potential in quantum dots is created by spatially extended charge distributions. Therefore, it shows a parabolic characteristic ( $\sim r^2$ ) and seems to represent fairly well the electrostatically confined electrons. The advantage of using a harmonic type of confining potential is the analytical simplicity of the problem since the center of mass and relative coordinates decouple. However, in the far-infrared spectroscopy, the radiation field can not detect the electron-electron correlations when the confinement is parabolic. This is caused by the decoupling of far-infrared radiation with the relative motion of electrons [24].

Thus, in order to probe the interaction effects, it has been suggested that the shape of the dot should be modified to achieve the coupling of center of mass and relative motions [24]. In [24], the heat capacity results have also been presented to suggest that the interaction effects could be seen by measuring the thermodynamic properties of the electrons. The magnetization of parabolic quantum dots has been also computed and magnetization found to be another probe of the interaction effects [25] like the heat capacity. The magnetization of the dots is predicted to oscillate with magnetic field because the ground state prefers to be at certain magic values of the total angular momentum. This behaviour is explained in a subsequent work [26] as a direct consequence of the Pauli principle which enables the electrons to reduce their energy optimally only at the magic angular momenta. Recently, vertically coupled quantum dots or artificial molecules [27,28] have attracted considerable attention. In [28], a double dot system with three spin-polarized electrons was investigated and a sequence of angular-momentum magic numbers was found depending on the strength of the interdot tunneling. Besides these, some authors have achieved the coupling of center of mass and relative motions of electrons with deviations from the exact harmonic confinement [29-31]. With etching techniques or self organized growth it is possible to create hard-wall type confinement potential [32]. Since the center of mass motion of electrons is coupled with their relative part in this type of confinement potential, the effects of correlation influencing energy spectrum, transport, and spectral measurements can be studied with the excitation spectra [33].

In this work we analyze electron correlation effects in a 2D circular quantum dot with hard wall confinement potential. We employ exact diagonalization technique in computing the

eigenvalues and corresponding eigenvectors for the ground state numerically. We specialize to the case of three spin-polarized electrons with total magnetic quantum number  $S_z = 3/2$  and total orbital angular momentum  $M = 0$ . We investigate charge density and pair correlation function as a function of the dot size under these circumstances. With increasing dot size the observed formation of Wigner molecule in equilateral triangular configuration of three electrons is discussed. In section 2 we give the formalism and details of the calculation. In section 3 and 4 we report and discuss the results of the numerical calculations.

## 2 Model and the method of calculation

The total orbital angular momentum  $M = \sum_{i=1}^N m_i$ , the total spin  $S$  and the total magnetic quantum number  $S_z = \sum_{i=1}^N s_i$  are good quantum numbers for  $N$  electrons in the dot due to the circular geometry of the dot, and spin independence of the Coulombic interaction. In second quantization language, the  $N$  electron quantum dot is described by the Hamiltonian

$$\mathcal{H} = \sum_K \mathcal{E}_K a_K^\dagger a_K + \frac{\lambda}{2} \sum_{K,L,M,N} V_{K,L,M,N} a_K^\dagger a_M^\dagger a_L a_N, \quad (1)$$

where  $\mathcal{E}_K = \frac{1}{2} k_{n_K, |m_K|}^2$  depends only on the  $n_K$ -th root of the Bessel function of the first kind  $J_{m_K}$ . In writing eqn. (1), length is measured in units of the dot radius  $a$ , and energy in units of  $\hbar^2/(m^* a_B^2 \lambda^2)$ , where  $m^*$  is the electron effective mass determined by the host semiconductor. In (1), the Coulomb potential is multiplied by  $\lambda = a/a_B$  which serves as the dimensionless coupling constant characterizing the strength of the interaction. Although it is possible to perform a perturbative expansion in powers of  $\lambda$  to calculate the energy spectrum [34], we prefer to diagonalize the Hamiltonian matrix exactly [33,35]. The Coulomb matrix element is defined via the one-electron orbitals as

$$V_{K,L,M,N} = \int \int d^2 \vec{x} d^2 \vec{x}' \varphi_K^*(\vec{x}) \varphi_L(\vec{x}) V(\vec{x} - \vec{x}') \varphi_M^*(\vec{x}') \varphi_N(\vec{x}'), \quad (2)$$

where  $\varphi_A(\vec{x})$  ( $A=K, L, M, N$ ) are the eigenfunctions of the single free particle Hamiltonian, and  $A$  is a collective index designating the radial ( $n_A$ ), angular momentum ( $m_A$ ) and spin quantum numbers ( $\sigma_A$ ) of the electron.  $\varphi_A(\vec{x})$  can be written as

$$\varphi_A(\vec{x}) = \phi_{n_A, m_A}(\vec{x}) \chi_{\sigma_A}, \quad (3)$$

where  $\chi_\sigma$  is the spin wavefunction, and one electron orbital  $\phi_{n,m}(\vec{x})$  has the form

$$\phi_{n,m}(\vec{x}) = \frac{1}{\sqrt{\pi}} \frac{1}{|J_{|m|+1}(k_{n,|m|}|\vec{x}|)} e^{im\theta} J_{|m|}(k_{n,|m|}|\vec{x}|), \quad (4)$$

and the corresponding eigenvalue  $\mathcal{E}_K$  is independent of both spin and sign of  $m$ . As the one electron orbitals depend already on the Bessel functions, it is convenient to expand the Coulomb potential,  $V(\vec{x} - \vec{x}') = \frac{1}{|\vec{x} - \vec{x}'|}$ , in terms of the Bessel functions,

$$\frac{1}{|\vec{x} - \vec{x}'|} = \sum_{m=-\infty}^{\infty} \int_0^{\infty} dk e^{im(\theta - \theta')} J_{|m|}(k\rho) J_{|m|}(k\rho') e^{-k(z_> - z_<)}, \quad (5)$$

where  $z_> - z_<$  shows the extension of the dot in the longitudinal direction. If the longitudinal extension of the dot is a non-negligible fraction of its in-plane size, one is to analyze the excitations in this direction, too. However, in the limit of  $z_> - z_< \rightarrow 0$ , it is sufficient to probe only the transversal plane assuming that the system is in the lowest state for longitudinal dynamics. In the following, we follow the latter one and ascribe a small value to  $z_> - z_<$  in the calculations. In this approximation the matrix element of the Coulomb potential becomes

$$\begin{aligned} V_{m_K, m_L, m_M, m_N}^{n_K, n_L, n_M, n_N} &= 4 \frac{1}{|J_{|m_K|+1}(k_{n_K, |m_K|})|} \frac{1}{|J_{|m_L|+1}(k_{n_L, |m_L|})|} \frac{1}{|J_{|m_M|+1}(k_{n_M, |m_M|})|} \\ &\frac{1}{|J_{|m_N|+1}(k_{n_N, |m_N|})|} \int_0^{\infty} dk \int_0^1 d\rho \rho J_{|m_K|}(k_{n_K, |m_K|} \rho) J_{|m_L|}(k_{n_L, |m_L|} \rho) \\ &J_{|m_K - m_L|}(k\rho) \int_0^1 d\rho' \rho' J_{|m_M|}(k_{n_M, |m_M|} \rho') J_{|m_N|}(k_{n_N, |m_N|} \rho') J_{|m_N - m_M|}(k\rho'). \end{aligned} \quad (6)$$

One notes that, angular integrations in  $V_{K,L,M,N}$  require  $m_K - m_L = m_N - m_M$  otherwise  $V_{K,L,M,N}$  vanishes.

For calculating the physical quantities such as energy spectrum, charge density and pair correlation function, one needs to compute the matrix elements of the Hamiltonian operator between N-electron ground state which can be expressed as

$$|\Phi_0^{(N)}\rangle = \sum_C b_C^0 |C\rangle, \quad (7)$$

where  $|C\rangle = a_{n_1, m_1, \sigma_1}^\dagger \dots a_{n_N, m_N, \sigma_N}^\dagger |0\rangle$  is a non-interacting Slater determinant and sum runs over all possible configurations of the quantum numbers  $(n, m, \sigma)$  satisfying given values of  $M$  and  $S_z$ . The expansion coefficients  $b_C^0$  are identified with the eigenvectors of the ground state. In this work we are concerned with the quartet ground state  $|S_z = 3/2, M = 0\rangle$

$$|S_z = 3/2, M = 0\rangle = a_{n_1, m_1, \uparrow}^\dagger a_{n_2, m_2, \uparrow}^\dagger a_{n_3, m_3, \uparrow}^\dagger |0\rangle, \quad (8)$$

in which all electrons are spin polarized. We will compute all relevant quantities in the quartet ground state.

The charge density of the electrons are defined by

$$\rho(\vec{x}) = \sum_{\sigma} \langle \Phi_0^{(N)} | \phi_{\sigma}^\dagger(\vec{x}) \phi_{\sigma}(\vec{x}) | \Phi_0^{(N)} \rangle, \quad (9)$$

which measures the electron density at a given point  $\vec{x}$  in space. A close inspection of this formula reveals that, at a fixed radius,  $\rho(\vec{x}) \sim \cos(2M\theta)$  so that angular dependence of the charge density is determined by the total orbital angular momentum. Hence, for  $M = 0$  angular dependence disappears and  $\rho(\vec{x})$  assumes only a radial variation dictated by the associated Bessel functions.

Another relevant quantity, the pair correlation function, is a two-point function defined by

$$\rho_c(\vec{x}, \vec{x}') = \sum_{\sigma, \sigma'} \langle \Phi_0^{(N)} | \phi_{\sigma}^{\dagger}(\vec{x}) \phi_{\sigma'}^{\dagger}(\vec{x}') \phi_{\sigma'}(\vec{x}') \phi_{\sigma}(\vec{x}) | \Phi_0^{(N)} \rangle, \quad (10)$$

which is the probability of finding an electron at  $\vec{x}$  given that another one is situated at  $\vec{x}'$ .

In the next section we perform a numerical computation of the charge density and pair correlation function to identify their dependence on the space coordinates as well as the dot size  $\lambda$ .

### 3 Numerical Analysis

Electron-electron correlations have been computed for a 1D hard-wall type dot in [36], and a 2D parabolic dot in [37]. In the latter the Schrodinger equation is solved for three electrons numerically for a fixed dot size. For three electrons with  $S_z = 3/2$  and  $M = 3k$  ( $k=0,1,2, \dots$ ) it is expected that, in the ground state, electrons form an equilateral triangle at some radius  $r_0$  determined by the confining parabolic potential. Here we analyze charge density and pair correlation function for three electrons in a circular quantum dot for  $S_z = 3/2$ ,  $M = 0$ . In contrast to the parabolic confinement potential, in the case of hard-wall type confinement one cannot find an analytic expression for  $r_0$ . Despite of this, however, for large enough  $\lambda$  value, the equilateral triangular configuration is expected to occur at some distance in the radial direction. This then will be an indication of the Wigner molecule structure which is a general feature of quantum dots for large  $\lambda$  [36].

Depicted in Fig.1 is the  $r$  and  $\lambda$  dependence of the charge density  $\rho(\vec{x})$  (normalized to  $N=3$  for each  $\lambda$ ) for the state  $|S_z = 3/2, M = 0 \rangle$ . The three curves in this figure describe variations of the electron distribution as a function of  $\lambda$  and  $r$ . For small  $\lambda$  (e. g.  $\lambda = 1$ ) electrons have non-negligible distribution at the center of the dot though maximum is reached away from the origin. This behaviour of  $\rho(\vec{x})$  shows that for small  $\lambda$   $J_{m=0}(r)$  is the dominant one especially at small  $r$ . As  $\lambda$  increases, however, the charge density vanishes gradually around the center of the dot (e. g.  $\lambda = 10, 100$ ). It is here that one observes the dominance of  $J_{m>0}$  since they vanish at the origin by definition. Besides the behaviour of the charge density close to the center of

the dot, one observes that higher the  $\lambda$  sharper and farther from the center the peaks become. Hence, as  $\lambda$  increases electrons get shifted towards the periphery (never reaching there due to the infinite potential barrier) with a sharper peak showing the most probable radial position of the electrons. For example, for  $\lambda = 100$  electrons are most probably distributed along the periphery at the radial distance  $r \sim 0.7$ . That electrons move towards the periphery with increasing  $\lambda$  follows from the fact that they try to minimize their electrostatic energy which is known to be the dominant component for large  $\lambda$ . Behaviour of the charge density gives information only on the radial distribution of electrons; therefore, one should also investigate the behaviour of the pair correlation function to obtain the distribution of the electrons in the plane of the dot.

In Fig.2 the variation of the pair correlation function (normalized to  $N(N-1)=6$ ) with  $\theta$  and  $\lambda$  for  $r = r' = 0.67$  and  $\theta' = 0$  is presented. The pair correlation function  $\rho_c(\vec{x}, \vec{x}')$  gives the probability distribution of  $N - 1$  electrons given that one of the  $N$  electrons is located at  $\vec{x}'$ . For the case of three electrons, the pair correlation function in Fig.2 shows the angular distribution of two electrons along the periphery of the quantum dot. Therefore, the fact that pair correlation function has always two distinct peaks and vanishes at  $\theta = 0$  is a restatement of the properties of the pair correlation function consistent with the Pauli exclusion principle.

An important property of the pair correlation function follows from its variation with the dot size in units of Bohr radius. One notices that, for small  $\lambda$  values peaks are not sharp and electrons do not have a well-defined configuration, that is, the pair correlation function is not diminished significantly between the two peaks. This small  $\lambda$  limit shows nothing but the atomic regime of confinement, where dot size is of the order of Bohr radius or smaller, and their average kinetic energy exceeds the Coulombic repulsion. It is with the dominant kinetic energy of the electrons that they are distributed in the dot without a well-defined configuration. It is known that in this limit perturbation theory is a reliable tool to investigate the physical parameters of the dot [38], in other words, Hartree-Fock method can be applied just as in the few-electron atoms.

Furthermore, as Fig. 2 shows clearly, when  $\lambda$  is increased peaks get sharper. Pair correlation function gradually assumes two distinct peaks between which there is a strong depletion. Therefore, higher the dot size smaller the overlap between the two peaks. Indeed, as  $\lambda$  increases the peaks approach to fixed positions such that their angular separation is  $\sim 120^\circ$ . This angular separation constitutes an equilateral triangular structure as already emphasized in other investigations too [37,38]. This geometrical arrangement of the electrons correspond

to the minimal energy configuration where their kinetic energy is smaller than the electrostatic Coulomb energy. The latter is minimized by an equilateral triangular configuration of the electrons. Approach of the configuration to an equilateral triangular structure for large dot sizes is nothing but the well-known Wigner molecule structure which has been shown to exist in other types of dots too [36,38]. Therefore, for large dot sizes one observes that the electrons form a Wigner molecule, that is, they assume fixed positions in the dot minimizing the dominant electrostatic energy.

For a better understanding of the behaviour of the electron distribution in the dot it may be convenient to analyze the pair correlation function in the  $r - \theta$  plane in which both radial and angular variations become visible. Fig. 3 shows the contour lines of  $\rho_c(\vec{x}, \vec{x}')$  in  $r - \theta$  plane for  $\theta' = 0$ ,  $r' = 0.67$ , and  $\lambda = 1$ . In accordance with Fig. 1 and Fig. 2 there is a non-negligible correlation between the electrons for small  $r$ , also the maxima are reached away from the origin,  $r \sim 0.4$ . Moreover near the periphery of the dot, the correlation distribution is highly suppressed. One also notices that the pair correlation function in between the two peaks is not suppressed at all.

To illustrate the effects of larger dot sizes on Fig. 3 we show in Fig. 4 the pair correlation function in  $r - \theta$  plane for  $\lambda = 100$ . As is seen there are important differences between Fig. 3 and Fig. 4. First of all, the peaks are pushed towards the periphery of the dot in comparison with Fig. 1. Next the peaks are now sharpened and the pair correlation between them are reduced significantly. In this sense the difference between Figs. 3 and 4 shows the crytallization process of the electrons with increasing Coulombic repulsion among them with growing  $\lambda$ .

## 4 Conclusion

In this work we have performed a detailed numerical study of the electron correlation effects in a 2D circular quantum dot with hard-wall confinement potential. Our investigations show that as the dot size increase gradually configuration of the electrons approach an equilateral triangular structure. Hard-wall quantum dots, which may be as interesting as parabolic ones for experimental studies, allow for the formation of the Wigner molecule structure of the electrons for large dot sizes compared to the Bohr radius. It is known that the optical properties like the inelastic light scattering or far infrared absorption [39] and magnetic properties are all dependent on the spin of the ground state. Therefore, experimental studies on the quantum dots can reveal valuable information on the electron configuration in the dot by concentrating on the spin dependent quantities.



## References

- [1] G. W. Bryant, Phys. Rev. Lett. **59** (1987) 1140.
- [2] M. A. Reed, J. N. Randall, J. Aggarwal, R. J. Matyi, T. M. Moore, and A. E. Wetsel, Phys. Rev. Lett. **60** (1988) 535.
- [3] W. Hansen, T. P. Smith III, K. Y. Lee, J. A. Brum, C. M. Knoedler, J. M. Hong, and D. P. Kern, Phys. Rev. Lett. **62** (1989) 2168; **64** (1990) 1991; W. Hansen, T. P. Smith III, K. Y. Lee, J. M. Hong, and C. M. Knoedler, Appl. Phys. Lett. **56** (1990) 168.
- [4] L. P. Kouwenhoven, F. W. J. Hekking, B. J. van Wees, C. J. P. M. Harmans, C. E. Timmering, and C. T. Foxon, Phys. Rev. Lett. **65** (1990) 361.
- [5] P. L. McEuen, E. B. Foxman, U. Meirav, M. A. Kastner, Y. Meir, N. S. Wingreen, and S. J. Wind, Phys. Rev. Lett. **66** (1991) 1926.
- [6] Ch. Sikorski and U. Merkt, Phys. Rev. Lett. **62** (1989) 2164; **64** (1990) 3100; Surf. Sci. **229** (1990) 282.
- [7] A. Lorke, J. P. Kotthaus, and K. Ploog, Phys. Rev. Lett. **64** (1990) 2559.
- [8] T. Demel, D. Heitmann, P. Grambow, and K. Ploog, Phys. Rev. Lett. **64** (1990) 788.
- [9] B. Meurer, D. Heitmann, and K. Ploog, Phys. Rev. Lett. **68** (1992) 1371.
- [10] W. Hausler and B. Kramer, Phys. Rev. **B47** (1993) 16353.
- [11] P. Hawrylak and D. Pfannkuche, Phys. Rev. Lett. **70** (1993) 485.
- [12] U. Merkt, J. Hausler, and M. Wagner, Phys. Rev. **B43** (1991) 7320.
- [13] W. Hausler, B. Kramer, and J. Masek, Z. Phys. **B85** (1991) 435.
- [14] D. Pfannkuche, V. Gudmundsson, and P. A. Maksym, Phys. Rev. **B47** (1993) 2244.
- [15] Y. Meir, N. S. Wingreen, and P. A. Lee, Phys. Rev. Lett. **66** (1991) 3048; J. M. Kinaret, Y. Meir, N. S. Wingreen, P. A. Lee, and X. G. Wen, Phys. Rev. **B46** (1992) 4681.
- [16] J. J. Palacios, L. Martin-Moreno, and C. Tejedor, Europhys. Lett. **23** (1993) 495.
- [17] S. R. Patel, D. R. Stewart, C. M. Marcus, M. Gokcedag, Y. Alhassid, A. D. Stone, C. I. Duruoz, and J. S. Harris, Jr, Phys. Rev. Lett. **81** (1998) 5900.

- [18] A. H. Guerrero, *Semi. Sci. Tech.* **10** (1995) 759.
- [19] E. A. Hylleraas, *Z. Phys.* **54** (1929) 347.
- [20] D. Babic, R. Tsu, and R. F. Greene, *Phys. Rev.* **B45** (1992) 14150.
- [21] P. Bakshi, D. A. Broido, and K. Kempa, *Phys. Rev.* **B42** (1990) 7416.
- [22] P. L. McEuen, N. S. Wingreen, E. B. Foxman, J. Kinaret, U. Meirav, M. A. Kastner, and Y. Meir, *Physica* **B189** (1993) 70.
- [23] U. Merkt, *Physica* **B189** (1993) 165.
- [24] P. A. Maksym and T. Chakraborty, *Phys. Rev. Lett.* **65** (1990) 108.
- [25] P. A. Maksym and T. Chakraborty, *Phys. Rev.* **B45** (1992) 1947.
- [26] P. A. Maksym, *Physica* **B184** (1993) 385.
- [27] B. Partoens, A. Matulis, and F. M. Peeters, *Phys. Rev.* **B59** (1999) 1617.
- [28] H. Imamura, P. A. Maksym, and H. Aoki, *Phys. Rev.* **53** (1996) 12613.
- [29] D. Pfannkuche and R. R. Gerhardts, *Phys. Rev.* **B44** (1991) 13132.
- [30] V. Gudmundsson and R. R. Gerhardts, *Phys. Rev.* **B43** (1991) 12098.
- [31] Z. L. Ye and E. Zaremba, *Phys. Rev.* **B50** (1994) 17217.
- [32] F. M. Peeters and V. A. Schweigert, *Phys. Rev.* **B53** (1996) 1468.
- [33] A. Brataas, U. Hanke, and K. A. Chao, *Semi. Sci. Tech.* **12** (1997) 825.
- [34] A. Matulis, J. O. Fjarestad, and K. A. Chao, *Physica Scripta* **T69** (1997) 85; **T69** (1997) 138.
- [35] N. Akman and M. Tomak, *Physica B*, to be published.
- [36] K. Jauregui, W. Hausler, and B. Kramer, *Europhys. Lett.* **24** (1993) 581.
- [37] X. -G. Li, W. -Y. Ruan, C. -G. Bao, and Y. -Y. Liu, *Few-Body Systems* **22** (1997) 91.
- [38] J. H. Jefferson and W. Hausler, preprint (cond-mat) 9705012.
- [39] A. Brataas, U. Hanke, and K. A. Chao, *Phys. Rev.* **B54** (1996) 10736.

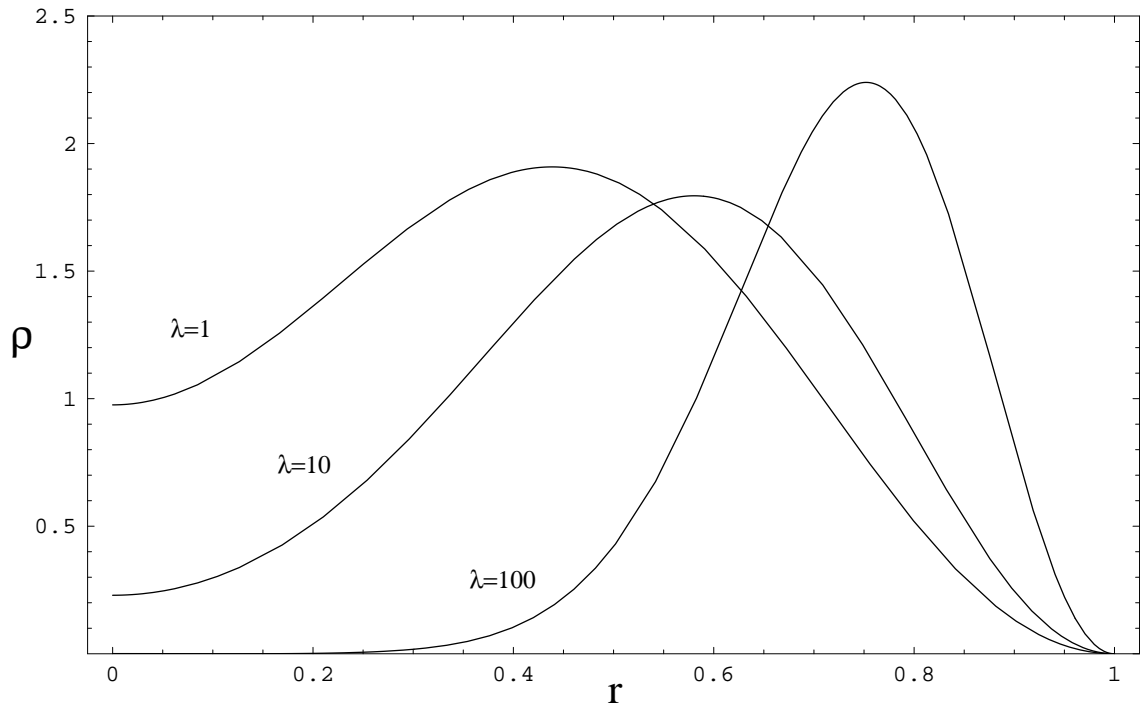
## Figure Captions

Fig. 1. Variation of the charge density  $\rho(\vec{x})$  with radial distance  $r$  and the dot size  $\lambda$ .

Fig. 2. Variation of the pair correlation function with  $\theta$  and  $\lambda$  for  $r = r' = 0.67$  and  $\theta' = 0$ .

Fig. 3. Contour lines showing the pair correlation function on  $(r - \theta)$  plane for  $r' = 0.67$ ,  $\theta' = 0$ , and  $\lambda = 1$ .

Fig. 4. The same as in Fig. 3 but for  $\lambda = 100$ .



**Fig.1**

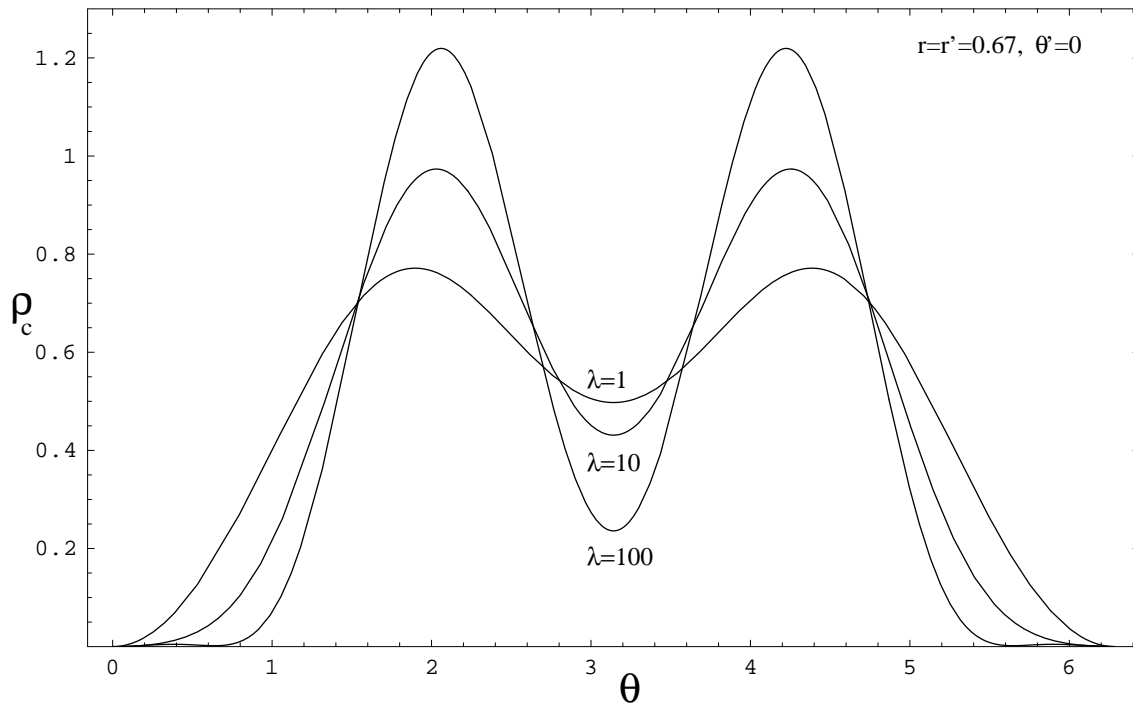
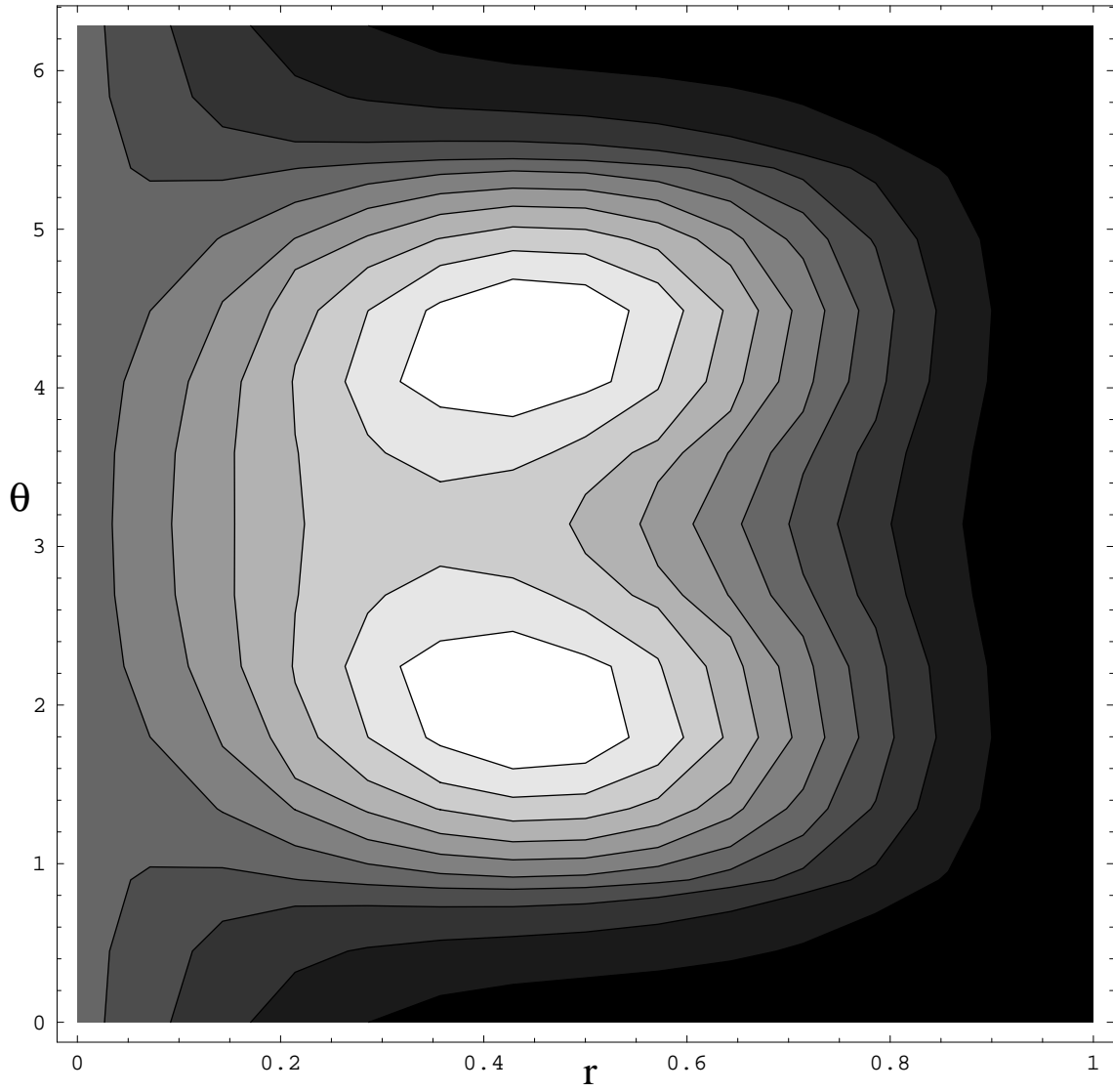


Fig.2



**Fig.3**

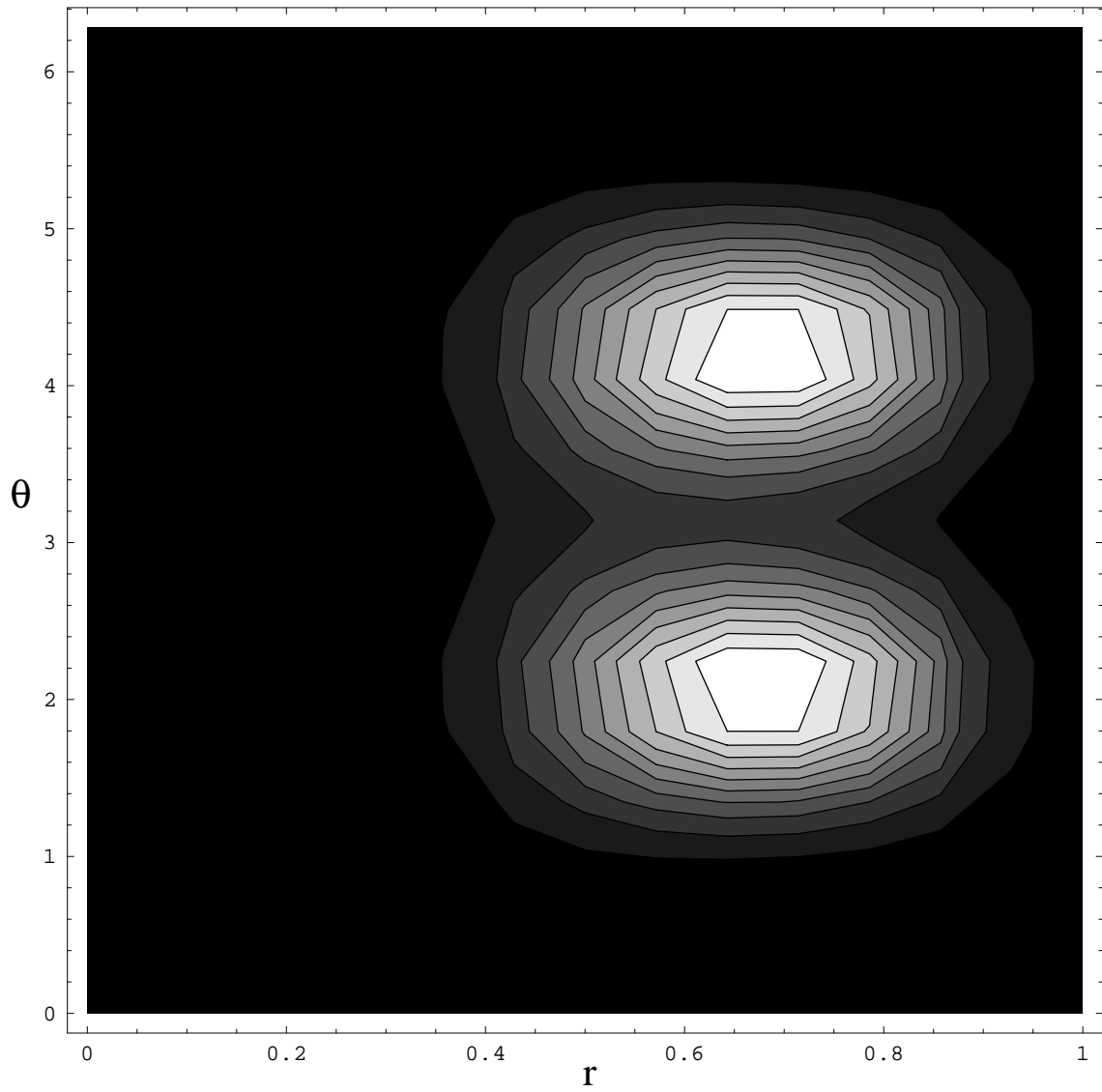


Fig.4

